

Document downloaded from:

<http://hdl.handle.net/10251/57088>

This paper must be cited as:

Ginzburg, P.; Rodríguez Fortuño, F.J.; Martínez Abietar, A.J.; Zayats, A.V. (2012). Analogue of the quantum Hanle effect and polarization conversion in non-hermitian plasmonic metamaterials. *Nano Letters*. 12(12):6309-6314. doi:10.1021/nl3034174.



The final publication is available at

<http://dx.doi.org/10.1021/nl3034174>

Copyright American Chemical Society

Additional Information

This document is the Accepted Manuscript version of a Published Work that appeared in final form in

Nano Letters, copyright © American Chemical Society after peer review and technical editing by the publisher. To access the final edited and published work see <http://pubs.acs.org/page/policy/articlesonrequest/index.html>

Analogue of the Quantum Hanle Effect and Polarization Conversion in Non-Hermitian Plasmonic Metamaterials

Pavel Ginzburg^{1*}, Francisco J. Rodríguez Fortuño^{1,2}, Alejandro Martínez² and
Anatoly V. Zayats¹

¹ Department of Physics, King's College London, Strand, London WC2R 2LS, United Kingdom

² Nanophotonics Technology Center. Universitat Politècnica de València. 46022 Valencia, Spain

The Hanle effect¹, being one of the first manifestations of quantum theory introducing the concept of coherent superposition between pure states, plays a key role in numerous aspects of science, varying from applicative spectroscopy² to fundamental astrophysical investigations^{3,4}. Optical analogues of quantum effects help to achieve deeper understanding of quantum phenomena and, in turn, to develop cross-disciplinary approaches to realizations of new applications in photonics^{5,6}. Here we show that metallic nanostructures can be designed to exhibit a plasmonic analogue of the quantum Hanle effect and its associated polarization rotation. In the original Hanle effect, the time-reversal symmetry is broken by a static magnetic field. Here we achieve this by introducing dissipative level crossing of localised surface plasmons due to nonuniform losses, as can be explained by a non-Hermitian formulation of quantum mechanics^{7,8}. These artificial plasmonic “molecules” arranged in ordered lattice are shown to form a new type of metamaterial with strong circular birefringence and optical activity.

*corresponding author: pavel.ginzburg@kcl.ac.uk

The quantum Hanle effect describes the polarization rotation of scattered electromagnetic radiation due to atomic coherence between Zeeman states, split by a weak magnetic field¹. The significance of this phenomenon is important in lifetime measurements and spectroscopy², detection of magnetic fields in solar prominence³ and stellar winds⁴. The main advantage for typical measurements of this kind is a very high spectral resolution and sensitivity to magnetic fields, since the level crossings are not limited by the Doppler width of the spectral lines, but solely by the coherence in individual atoms. The observation of the Hanle effect is possible in the presence of a magnetic field which violates the time-reversal symmetry as was observed in the experiments on coherent backscattering⁹ and can contribute to parity symmetry breaking¹⁰.

The investigations of optical analogues of quantum effects are important to achieve deeper understanding of quantum phenomena and give prospect to new applications based on cross-disciplinary approaches. For example, the realization of sharp spectral resonances with nanoscale metallic (plasmonic) nanostructures important for biosensing and nonlinear photonic applications has resulted from the studies of optical counterparts of the Fano resonance (interference between scattering amplitudes of bound and continuum electronic states)⁵ and electromagnetically induced transparency (EIT) (destructive interference of electron probability amplitudes, induced by two spectrally different optical beams)⁶.

Here we investigate an optical counterpart of the quantum Hanle effect. By employing the concepts of nonhermitian quantum mechanics^{7,8}, we have designed an artificial plasmonic “atom” which has a pair of degenerate resonances that split by

broken time-reversal symmetry due to the presence of loss. This is a complete optical analogue of the atomic system where initially degenerate atomic states are split when the time-reversal symmetry is broken by the magnetic field¹. Two-dimensional (2D) arrays of these particles can form a new artificial material (metamaterial) with extremely efficient optical activity.

Metamaterials provide vast opportunities to manipulate light beams in an uncommon way¹¹, promising a wide range of potential applications such as cloaking^{12,13} and perfect lensing¹⁴ based on negative index of refraction. In the optical range, the properties of metamaterials rely on plasmonic effects¹¹. In this work we will employ the localized surface plasmon (LSP) resonances supported by metal nanoparticles made of noble metals¹⁵. These resonances are solely determined by the particle's shape and surrounding environment and can be engineered and tuned to the desired frequency^{16–18}.

The basic scheme of the Hanle effect is represented in Fig. 1(a-b). Linearly polarized light, being a superposition of left and right circular polarizations, excites coherently the p-orbitals of an atom, conserving the total angular momentum. The degeneracy between p-states [Fig. 1(a)] could be removed by an applied static magnetic field [Fig 1(b)]. The excited p-states evolve in time with slightly dissimilar time constants, adding different phases for opposite circular polarizations and, as a consequence, resulting in polarization-unpreserved light scattering. The polarization of the scattered light depends then on the strength of the magnetic field. The plasmonic “atom level” diagram of our optical analogue is shown in Fig. 1(c-d). The vacuum state ($|\text{vac}\rangle$) is analogous to the ground state of an atom, while the degenerate (in frequency) LSP resonances represent the p-orbitals of this atom and are marked as $|H\rangle$ and $|V\rangle$ on the diagram [Fig. 1(c)]. The degeneracy of this LSP

states can be removed by dissipative coupling in the presence of nonuniform loss [Fig. 1(d)], resulting in the shift of LSP resonances with respect to each other, as will be shown below.

The nanoparticle analysed in this work has been taken to be a metallic cross that has two degenerate dipolar LSP resonances, corresponding to horizontal ($|H\rangle$) and vertical ($|V\rangle$) polarisations, respectively. This particle is used as the unit cell of the array depicted in Fig. 1(e), and it represents the above description when $\epsilon_{im}=0$. In this degenerate case, the polarisation of the normally incident light on the nanostructure will not change. In principle, degeneracy may take place between plasmonic resonances of any order and could lead to interesting interplay and time evolution¹⁹. The degeneracy between the LSP resonances can be removed by introduction of losses (imaginary part of permittivity $\epsilon_{im}\neq 0$) in some places near the cross arms. Such plasmonic nanoparticle with non-degenerate $|H\rangle$ and $|V\rangle$ states coherently scatters a fraction of the incident linearly polarised light into the orthogonal polarization state. Thus, the polarisation of the scattered light will depend on the “splitting” of the LSP states governed by the loss—in analogy to the polarisation state of light scattered by atoms in the quantum Hanle effect depending on the splitting of atomic levels governed by magnetic field.

To analyze the loss-induced interplay and coupling between eigenmodes of the structure we developed a rigorous theoretical description using the non-Hermitian quantum mechanical approach to describe loss-induced coupling between LSP resonances^{7,8}. Non-Hermitian formulation of quantum mechanics is especially useful in the description of dissipative systems helping to get rid of ‘bath’ degrees of freedom. Rigorously, probability conservation does not necessarily mean the hermiticity of time-evolution operators, but just the combination of parity and time-

reversal commutations with an appropriate Hamiltonian of the system. Interesting phenomena, such as higher harmonics generation²⁰ or unidirectional mode coupling in waveguide structures²¹, may be analyzed in terms of this nonhermitian formalism. For our plasmonic system –or any other electromagnetic system under consideration- the eigenmodes can be derived from the solution of the following master equations²²:

$$\begin{aligned}\Theta\bar{H}(\vec{r}) &= \left(\frac{\omega}{c}\right)^2 \bar{H}(\vec{r}) \\ \Theta(\bar{H}(\vec{r})) &= \nabla \times \left[\frac{1}{\varepsilon(\vec{r}, \omega)} \nabla \times \bar{H}(\vec{r}) \right],\end{aligned}\tag{1}$$

where $\bar{H}(\vec{r})$ is the magnetic field of the mode, ω is the angular frequency, c is the speed of light in vacuum, and $\varepsilon(\vec{r}, \omega)$ is the position and frequency dependent dielectric constant. If both dispersion and absorption of the medium are neglected, the above defined Θ -operator is Hermitian and forms a complete orthogonal set of eigenmodes $\{\bar{H}(\vec{r})\}$. Nevertheless, for certain problems (e.g. lasers, optical amplifiers or lossy structures), even if a single frequency is considered, the dielectric permittivity is a complex number and the Θ -operator is not Hermitian anymore. However, it is always possible to decompose it into a sum of Hermitian and anti-Hermitian parts as follows:

$$\begin{aligned}
\Theta(\bar{H}(\vec{r})) &= \Theta_H(\bar{H}(\vec{r})) + \Theta_A(\bar{H}(\vec{r})) \\
\Theta_H(\bar{H}(\vec{r})) &= \nabla \times \left[\frac{\varepsilon_r(\vec{r}, \omega)}{\varepsilon_r^2(\vec{r}, \omega) + \varepsilon_{im}^2(\vec{r}, \omega)} \nabla \times \bar{H}(\vec{r}) \right] \\
\Theta_A(\bar{H}(\vec{r})) &= -i \nabla \times \left[\frac{\varepsilon_{im}(\vec{r}, \omega)}{\varepsilon_r^2(\vec{r}, \omega) + \varepsilon_{im}^2(\vec{r}, \omega)} \nabla \times \bar{H}(\vec{r}) \right],
\end{aligned} \tag{2}$$

where Θ_H and Θ_A are the Hermitian and anti-Hermitian operators and $\varepsilon(\vec{r}, \omega) = \varepsilon_r(\vec{r}, \omega) + i\varepsilon_{im}(\vec{r}, \omega)$. Θ_H provides an orthogonal set of eigenmodes spanning the entire electromagnetic space.

In the following we have considered (for the sake of simplicity) only two modes $|a\rangle$ and $|b\rangle$, investigating their coupling originating from the presence of loss or gain ($\Theta_A \neq 0$). The total magnetic field is given by the sum of individual modes:

$$\bar{H}(\vec{r}) = a(t)\bar{H}_a(\vec{r})e^{i\omega t} + b(t)\bar{H}_b(\vec{r})e^{i\omega t}, \tag{3}$$

where $a(t)$ and $b(t)$ are the complex time-dependent amplitudes of each mode. In the case of small imaginary part of the permittivity ($\varepsilon_r(\vec{r}, \omega) \gg \varepsilon_{im}(\vec{r}, \omega)$), the time evolution can be obtained in the slowly varying amplitudes ($a(t), b(t)$) approximation by inserting Eq.3 into Eq.2 and taking into account the orthogonality of the field components ($\int \bar{H}_i^*(\vec{r}) \cdot \bar{H}_j(\vec{r}) d^3\vec{r} = \frac{\hbar\omega}{2\mu_0} \delta_{ij}$):

$$\begin{aligned}
\frac{da(t)}{dt} &= -\xi_a a(t) - \xi_{ab} b(t) \\
\xi_a &= \frac{\varepsilon_0}{\hbar} \int \varepsilon_{im}(\vec{r}) \vec{E}_a^*(\vec{r}) \vec{E}_a(\vec{r}) d^3\vec{r} \\
\xi_{ab} &= \frac{\varepsilon_0}{\hbar} \int \varepsilon_{im}(\vec{r}) \vec{E}_a^*(\vec{r}) \vec{E}_b(\vec{r}) d^3\vec{r}
\end{aligned} \tag{4}$$

where $\vec{E}_j(\vec{r})$ is the electric field corresponding to the j -th mode and \hbar is the Plank constant. A similar equation may be obtained for the amplitude of the mode $b(t)$.

As can be seen from Eq. 4, the coupling between the two modes is given by an overlap integral weighed by the space-dependent imaginary part of the permittivity. For structures with high symmetry and uniform losses, the coupling coefficients between two modes will be identically zero. However, the situation will be completely different if the medium is not uniformly lossy (e.g., selectively doped dielectric substrate or electrically or optically induced loss or gain). The loss-induced coupling will cause the removal of the degeneracy and will lead to the modification of the polarisation state of scattered light (Fig. 1(d)).

In order to validate the analytical results, we have numerically simulated gold nano-crosses on a silica substrate, surrounded by a host dielectric medium. This surrounding material has been chosen to be selectively lossy only in one quarter of space (Fig. 1(e)). The metallic particles were distributed in an ordered array with 600 nm periodicity, forming a 2D planar metamaterial structure in order to enhance the overall optical response. The particle dimensions (marked on Fig. 1(e)) were taken to be $w = 100$ nm, $t = 20$ nm, and $l = 400$ nm. The refractive index of the substrate, as well as embedding dielectric is 1.45, while the losses in one quarter of the

embedding dielectric are subject to changes. A Drude model fit for gold was chosen for the particle's material²³.

The numerical experiment was performed in the frequency domain using the commercial software CST Microwave StudioTM with periodic boundary conditions. The normalized transmission spectra for amplitudes (upper set of curves in Fig. 2(a)) are shown for the metamaterial with different losses of the dielectric patch (Fig. 1 (e)). With the increased loss, the LSP resonances exhibit broadening as expected. The level splitting between $|H\rangle$ and $|V\rangle$ states cannot be observed in these transmission spectra due to the natural broadening of the resonances. The width of the resonances is determined by the coefficients ξ_a and ξ_b (Eq. 4) which depend on both metal and dielectric losses, while the level splitting is defined by the coupling coefficient - ξ_{ab} . Assuming a passive environment ($\epsilon_{im}(\vec{r}) > 0$), the weighted Hermitian inner product over L^2 metric space may be defined, and the following Cauchy-Schwarz inequality will hold

$$\xi_a \xi_b \geq |\xi_{ab}|^2 . \quad (5)$$

This implies that in this system the broadening of the resonances with the loss increase will always be greater than the splitting, preventing the direct observation of the splitting of the resonances. This is in striking contrast with the plasmonic analogues of EIT⁶, where the splitting is larger than the resonance width. In our case the coupling takes place between two “bright” modes while a “dark” (with narrow linewidth) mode is generally used for EIT. The splitting can be observed, however, if we consider the transmission spectra for the two uncoupled supermodes of the unit cell, $|V\rangle+|H\rangle$ and $|V\rangle-|H\rangle$, which result from the coupling of $|H\rangle$ and $|V\rangle$. These two

supermodes can be excited independently using incident diagonal polarizations, for which two different resonances in the transmission spectra can be seen (Fig. 2(c)), with no polarization conversion between them. We see in Fig. 2(c) that the splitting of the two supermodes increases with the losses, as predicted by our model.

The lower set of curves in Fig. 2(a) shows the conversion efficiency of the polarization defined as the ratio of the square root of intensity of V-polarized (scattered) to H-polarized (incident) fields. The overall conversion efficiency is reaching 10% in the vicinity of the LSP resonance and may be improved by increasing losses (Fig. 2b).

The steady state behaviour of the system may be analyzed in terms of ‘rate equations’ following the energy diagram in Fig. 1(d). The mode population of the vertical (V) resonance under the incident horizontal (H-polarized) field is obtained as:

$$\begin{aligned}
 V &= \kappa \frac{\xi_{ba} (\gamma_{V,rad} + \gamma_{V,dis}) (\gamma_{H,rad} + \gamma_{H,dis})}{\xi_{ba} \xi_{ab} (\gamma_{V,rad} + \gamma_{V,dis}) (\gamma_{H,rad} + \gamma_{H,dis}) - 1} E \approx \\
 &\approx -\kappa \xi_{ba} (\gamma_{V,rad} + \gamma_{V,dis}) (\gamma_{H,rad} + \gamma_{H,dis}) E
 \end{aligned} \tag{6}$$

where E is the input H-polarized field amplitude and $\gamma_V = \gamma_{V,rad} + \gamma_{V,dis}$, being $\gamma_{V,rad}$ and $\gamma_{V,dis}$ the radiative and nonradiative (dissipative) lifetimes, respectively. In the approximation made in Eq. 5, we assumed that the inter-mode coupling (ξ_{ab}) is small compared to the overall damping coefficient which is proportional to ξ_a and ξ_b (Eq. 4). The far-field intensity of light with the rotated polarization is proportional to $V / \gamma_{V,rad}$. The behaviour of the conversion efficiency with ξ_{ab} , predicted to be linear

by Eq. 6, is verified by the numerical experiment for small losses where Eq. (6) is valid, and deviates slightly from linear dependence at larger losses (Fig. 2(b)).

It is interesting to consider the effect that this structure has on incident circular polarization. The output transmitted polarization (the amplitude ratio and the phase difference between the vertical and horizontal components) is plotted in Fig. 3(a), both for incident right- and left-handed circular polarization. We see that elliptical polarization is transmitted near the resonance. The reflected polarization is also elliptical (Fig 3(b)). The degree of ellipticity also depends on how close the wavelength of the incident light is to the plasmonic resonances and on the loss.

We have introduced an analogue of the quantum Hanle effect in artificial plasmonic molecules. Ordered arrays of artificial molecules are shown to form a metamaterial with extraordinary pronounced circular birefringence and optical activity induced by loss-coupled polarisation states. The efficient control of the polarization state of light can be achieved using this effect in subwavelength thick slabs in both reflection and transmission geometries. Polarization manipulation by 2D optically active artificially structured media has been previously demonstrated in several configurations, such as planar arrays of subwavelength gammadions²⁴, spiral bull-eye structures²⁵, and 3D metamaterials²⁶. The use of the loss-coupled states open the possibility to build metamaterial components for active control of the reflected or transmitted light polarization if the nonuniform loss can be selectively induced by external stimuli, such as thermal, electric or optical signals. If turned around, the effect can be used for measurements of local absorption (or gain) in metamaterials via polarization measurements or indeed in sensing applications for analytes introducing optical loss. Understanding of spatially nonuniform loss/gain coupling is imperative also for the development of loss-compensation and gain in

metamaterials, where loss may result in additional and sometimes undesirable effects. From the fundamental point of view, the proposed general formalism for dissipative level crossing by employing the non-Hermitian effects in metamaterials may be used to analyse and design new effects in plasmonic systems where metal loss is intrinsically present.

Acknowledgments. This work has been supported in part by EPSRC (UK). P. Ginzburg acknowledges Royal Society for a Newton International Fellowship. F. J. Rodríguez-Fortuño acknowledges support from grant FPI of GV and the Spanish MICINN under contracts CONSOLIDER EMET CSD2008-00066 and TEC2011-28664-C02-02.

Figure Captions

Figure 1. Quantum Hanle effect and its plasmonic analogue. (a-b) Basic level structure of ‘traditional’ Hanle effect (a) without and (b) with an applied magnetic field to break time symmetry. (c-d) Optical counterpart of the Hanle effect in an artificial plasmonic molecule: (c) Degenerate resonances in the symmetric particle and (d) dissipative coupling of the resonances $|H\rangle$ and $|V\rangle$ (top) and its equivalent scenario of the splitting into two supermodes $|V\rangle+|H\rangle$ and $|V\rangle-|H\rangle$ (bot). (e) Schematic of the metamaterial unit cell for the observation of the Hanle effect analogue: a metal nanocross on a substrate, with an embedding dielectric, one quarter of which will have the imaginary part of the permittivity subject to changes.

Figure 2. Spectral response and polarization conversion. (a) (upper set of curves) S-parameter transmission spectra, (lower curves) polarization conversion efficiency, defined as the s-parameter transmission from the input to the orthogonal polarization at the output. The different loss values for one quarter of the embedding dielectric appear at the legends. (b) Polarization conversion efficiency as a function of induced losses. (c) Transmission spectra for the two incident diagonal polarization exciting the two uncoupled supermodes of the structure, showing the increased splitting for higher loss values of the dielectric patch. In all the spectral figures, the transmission s-parameter is plotted, defined as $S_T = (E_{out} / \sqrt{\eta_s}) / (E_{in} / \sqrt{\eta_0})$ where η_s and η_0 are the substrate and vacuum wave impedances, such that the power transmission is given by $T = |S_T|^2$. We use s-parameters rather than power transmission because, being proportional to the electric field amplitude, they are easily related to field polarization.

Figure 3. Effects on incident circular polarization. Amplitude ratio (solid line) and phase difference (dashed line) of the vertical and horizontal (a) transmitted field components and (b) reflected field components, when the input plane wave is right or left-handed circularly polarized.

References

1. Hanle, W. Über magnetische Beeinflussung der Polarisation der Resonanzfluoreszenz. *Zeitschrift für Physik A Hadrons and Nuclei* **30**, 93–105 (1924).
2. Colegrove, F., Franken, P., Lewis, R. & Sands, R. Novel Method of Spectroscopy With Applications to Precision Fine Structure Measurements. *Physical Review Letters* **3**, 420–422 (1959).
3. Stenflo, J. O. The Hanle effect and the diagnostics of turbulent magnetic fields in the solar atmosphere. *Solar Physics* **80**, 209–226 (1982).
4. Ignace, R., Nordsieck, K. H. & Cassinelli, J. P. The Hanle Effect as a Diagnostic of Magnetic Fields in Stellar Envelopes. I. Theoretical Results for Integrated Line Profiles. *The Astrophysical Journal* **486**, 550–570 (1997).
5. Luk'yanchuk, B. *et al.* The Fano resonance in plasmonic nanostructures and metamaterials. *Nature materials* **9**, 707–15 (2010).
6. Liu, N. *et al.* Plasmonic analogue of electromagnetically induced transparency at the Drude damping limit. *Nature materials* **8**, 758–62 (2009).
7. Moiseyev, N. *Non-Hermitian Quantum Mechanics*. (Cambridge University Press: 2011).
8. Bender, C. M. Making sense of non-Hermitian Hamiltonians. *Reports on Progress in Physics* **70**, 947–1018 (2007).
9. Labeyrie, G. *et al.* Hanle Effect in Coherent Backscattering. *Physical Review Letters* **89**, (2002).
10. MacKintosh, F. & John, S. Coherent backscattering of light in the presence of time-reversal-noninvariant and parity-nonconserving media. *Physical Review B* **37**, 1884–1897 (1988).
11. Sarychev, A. K. & Shalaev, V. M. *Electrodynamics of Metamaterials*. (World Scientific: Singapore, 2007).
12. Schurig, D. *et al.* Metamaterial electromagnetic cloak at microwave frequencies. *Science* **314**, 977–80 (2006).
13. Cai, W., Chettiar, U. K., Kildishev, A. V. & Shalaev, V. M. Optical cloaking with metamaterials. *Nature Photonics* **1**, 224–227 (2007).

14. Pendry, J. B. Negative Refraction Makes a Perfect Lens. *Physical Review Letters* **85**, 3966–3969 (2000).
15. Maier, S. A. *Plasmonics: Fundamentals and Applications*. (Springer: 2010).
16. Berkovitch, N., Ginzburg, P. & Orenstein, M. Concave plasmonic particles: broad-band geometrical tunability in the near-infrared. *Nano letters* **10**, 1405–8 (2010).
17. Prodan, E., Radloff, C., Halas, N. J. & Nordlander, P. A hybridization model for the plasmon response of complex nanostructures. *Science* **302**, 419–22 (2003).
18. Berkovitch, N., Ginzburg, P. & Orenstein, M. Nano-plasmonic antennas in the near infrared regime. *Journal of physics. Condensed matter: an Institute of Physics journal* **24**, 073202 (2012).
19. Ginzburg, P., Berkovitch, N., Nevet, A., Shor, I. & Orenstein, M. Resonances on-demand for plasmonic nano-particles. *Nano letters* **11**, 2329–33 (2011).
20. Gilary, I., Kaprálová-Žďánská, P. & Moiseyev, N. Ab initio calculation of harmonic generation spectra of helium using a time-dependent non-Hermitian formalism. *Physical Review A* **74**, (2006).
21. Ginzburg, P., Hayat, A., Vishnyakov, V. & Orenstein, M. Photonic logic by linear unidirectional interference. *Optics Express* **17**, 4251 (2009).
22. Joannopoulos, J. D., Johnson, S. G., Winn, J. N. & Meade, R. D. *Photonic Crystals: Molding the Flow of Light*. (Princeton University Press: 2008).
23. Johnson, P. B. & Christy, R. W. Optical Constants of the Noble Metals. *Physical Review B* **6**, 4370–4379 (1972).
24. Papakostas, A. *et al.* Optical Manifestations of Planar Chirality. *Physical Review Letters* **90**, (2003).
25. Drezet, A., Genet, C., Laluet, J.-Y. & Ebbesen, T. W. Optical chirality without optical activity: How surface plasmons give a twist to light. *Optics Express* **16**, 12559 (2008).
26. Zhao, Y. & Alù, A. Manipulating light polarization with ultrathin plasmonic metasurfaces. *Physical Review B* **84**, (2011).

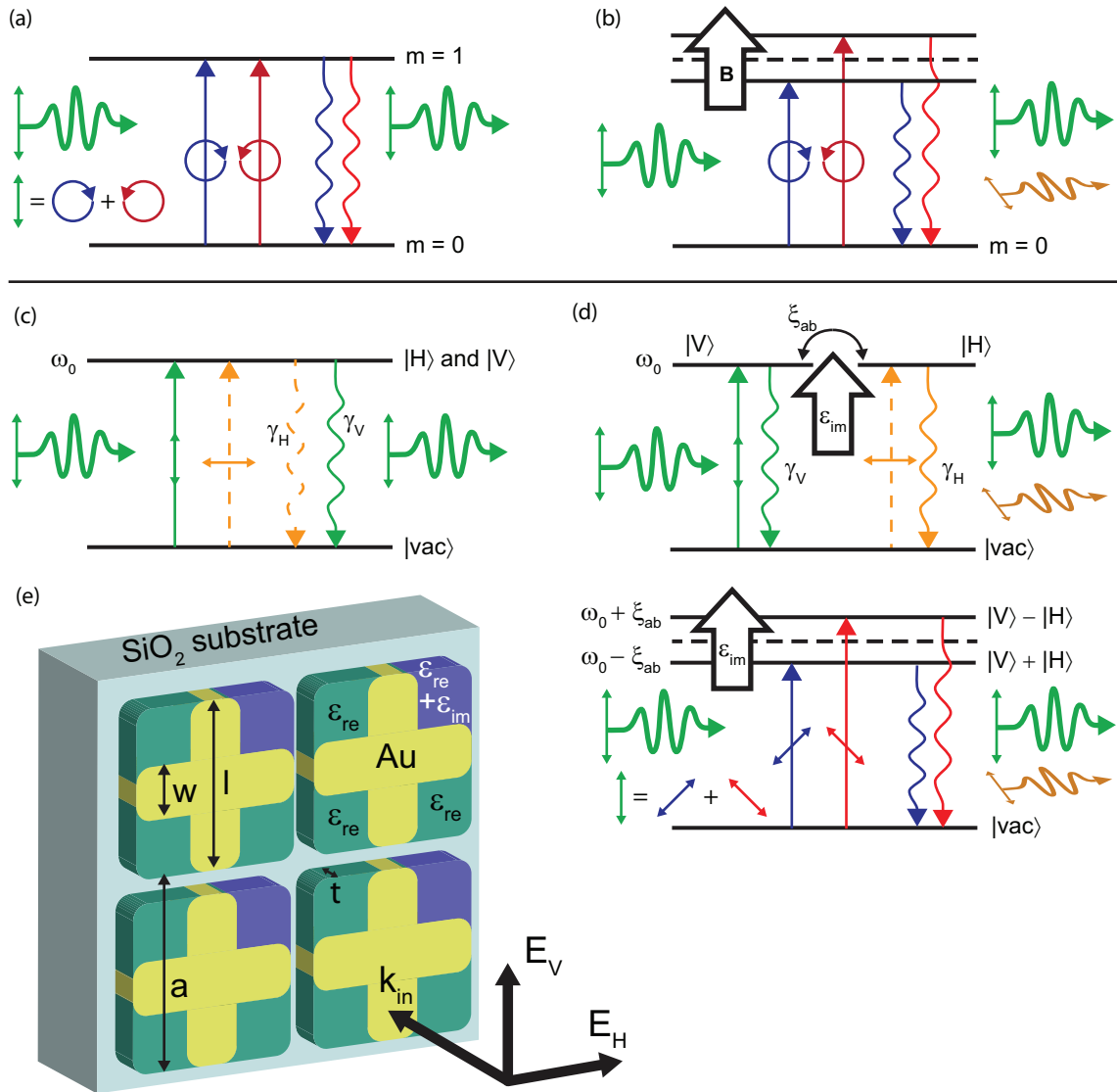


Figure 1. Quantum Hanle effect and its metamaterial analogue.

(this is a double column figure)

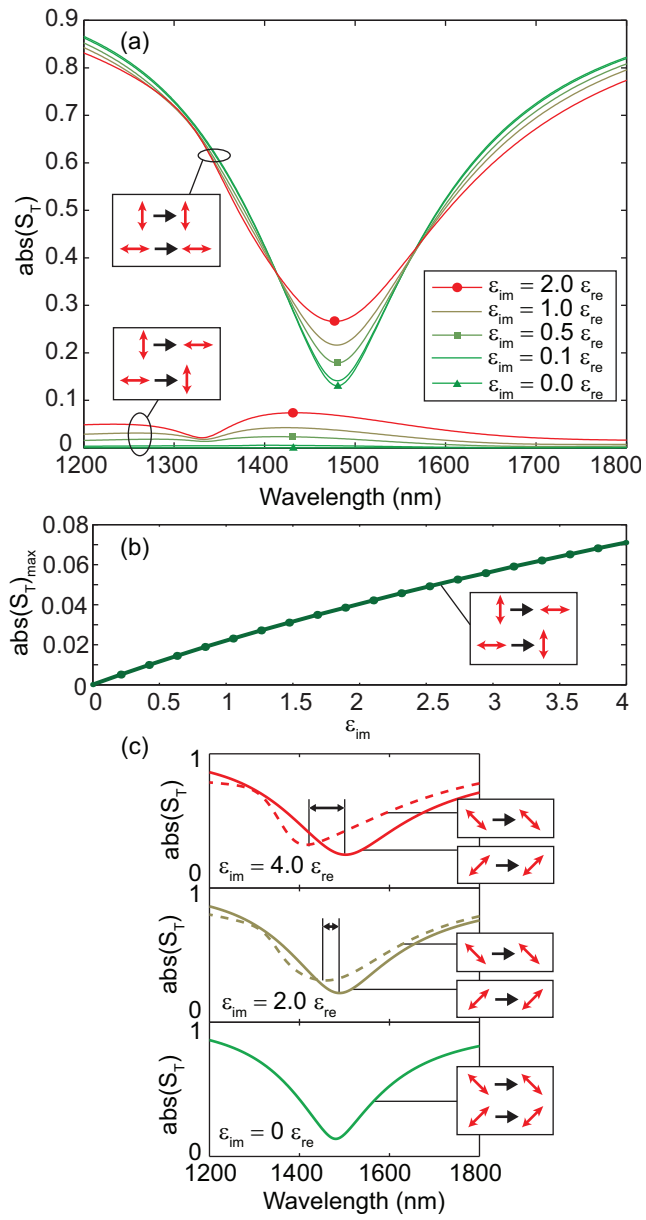


Figure 2. **Spectral response and polarization conversion**

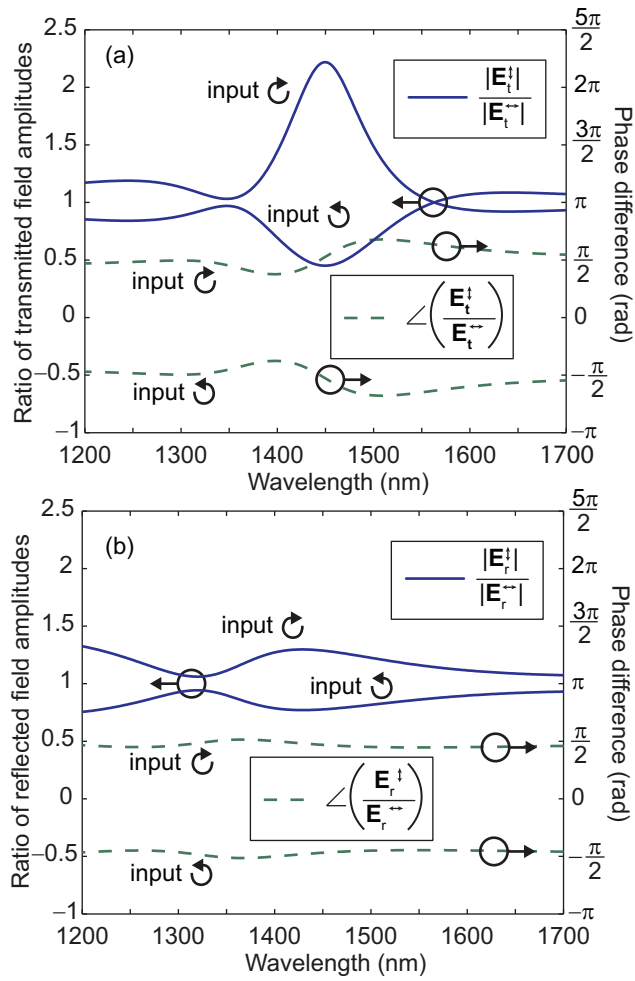


Figure 3. Effects on incident circular polarization.